

WIND EFFECT ANALYSIS ON AIR TRAFFIC CONGESTION IN TERMINAL AREA VIA CELLULAR AUTOMATA

Fatemeh ENAYATOLLAHI , M. A. AMIRI ATASHGAH *

*Faculty of New Sciences and Technologies, University of Tehran, North Amirabad Street,
1417466191, Tehran, Iran*

Received 02 May 2018; accepted 23 September 2018

Abstract. The behavior of any traffic flow is sensitive to the speed pattern of the vehicles involved. The heavier the traffic, the more sensitive the behavior is to speed changes. Focusing on air traffic flow, weather condition has a major role in the deviations of aircraft operational speed from the desired speed and causes surplus delays. In this paper, the effects of wind on delays in a terminal area are analyzed using a Cellular Automaton (CA) model. Cellular automata are discrete models that are widely used for simulating complex emerging properties of dynamic systems. A one-dimensional cellular array is used to model the flow of the terminal traffic into a wind field. The proposed model, due to the quickness and acceptable level of accuracy, can be utilized online in the tactical phase of air traffic control processes and system-level decision-makings, where quick response and system behavior are needed. The modeled route is an RNAV STAR route to Atlanta International Airport. The model is verified by real traffic data in a non-delayed scenario. Based on simulation results, the proposed model exhibits an acceptable level of accuracy (3-15% accuracy drop), with worthy time and computational efficiency (about 2.9 seconds run time for a 2-hour operation).

Keywords: terminal area traffic, traffic flow management, wind effect, traffic modeling, cellular automata.

Introduction

Global population growth and economic development around the world increase the need for land and aerial transportation systems. Studies show that the number of passenger-miles has doubled during the past decade and the number of aircraft flying over the globe will double by 2032 (Airbus, 2013). Considering aircraft types and load factors, the number of passengers is expected to triple in the next 20 years. On the other hand, reports show that in 2008 in the United States alone, air traffic delays caused the loss of more than 40.7 billion dollars (Schumer, 2008). Therefore, the delay is considered as an important performance index for the air transportation system. To this end, studies regarding delay initiation and propagation in the air traffic management (ATM) system as well as solutions to reduce the delays have received great attention in recent years. Delays may occur due to technical, operational or meteorological issues. As operations continue, these delays can propagate, magnify and affect considerable parts of the system. According to the FAA report, as seen in Figure 1, the weather caused more than 69% of

the system-affecting-delays over the six years from 2008 to 2013 in the United States (Federal Aviation Administration [FAA], 2017). Furthermore, this report states that airport winds in the terminal area contribute to up to 20% of the weather delays. In order to study this effect in the terminal area, a simple yet capable model is needed. An efficient model could also be used online in tactical phases of air traffic control processes.

OPSNET Standard Reports, Delay by Cause, 2008-2013

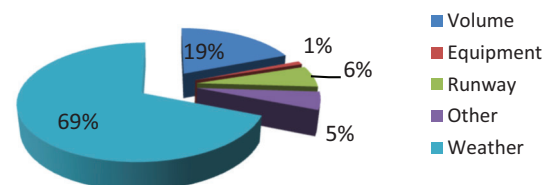


Figure 1. Delay by Cause Report in the United States (FAA, 2017)

*Corresponding author. E-mail: atashgah@ut.ac.ir

Traffic flow models, based on their approach, can be categorized into two groups: micro and macro models. Micro-models are trajectory based. They consider each vehicle as an individual particle and solve equations of motion for each one separately and in conjunction with other particles. This makes the complexity of calculations dependent upon the size of the problem and the number of involved particles, which is numerically intensive for large-scale modeling. Queuing network models (Jacobsen, 2000; Yang & Menon, 2015) and Lagrangian flow theory models (Bilimoria, 2001) are examples of micro models. In contrast, macro models consider a volume of the space under study and analyze performance indices and other characteristics of the flow regardless of each particle's trajectory. These models are capable of projecting the flow distribution as a function of space and time. Also, the fact that the complexity of calculations in macro models is independent of the number of vehicles makes them suitable approaches in system-level studies, where micro models are more applicable in aircraft-level works. Eulerian models, inspired by Euler flow theory (Bai & Menon, 2013; Menon, Sweriduk, & Bilimoria, 2004; Menon, Sweriduk, Lam, Diaz, & Bilimoria, 2006) and (Bayen, Raffard, & Tomlin, 2004; Pasaoglu, Baspinar, Ure, & Inalhan, 2015; Zhang, Xu, Yang, & Liu, 2014), are well-developed macro models for highway and air traffic flows. Cellular Automata (CA) are able to represent both Lagrangian and Eulerian approaches and benefit from the advantages of each group (Matsukidaira & Nishinari, 2004). With a considerably simple structure, CA can reproduce randomness and complex behaviors. Sun, Strub, and Bayen (2007) give a comparison of computational performance indices of these approaches. The indices used for their assessment are absolute and relative errors of the results for accuracy, CPU time, and RAM usage for computational efficiency of the models. The underlying simplicity in the CA structure supports the computational efficiency of the model with reasonable accuracy. The degree of accuracy increase depends on the space and time discretization method and the level and definition of model resolution. Sun et al. (2007) show that the CA model can reach a comparable level of accuracy compared to the PDE model and Eulerian flow theory models in about 0.1 of their CPU time. This level of time-efficiency, together with acceptable error, makes CA models a worthy candidate for simulations in pre-tactical and tactical phases of air traffic control that include days up to hours before operations. In addition, one may categorize models based on whether they use continuous or discrete time, space, and states. In other words, some methods use a continuous time approach while some others use discrete time, and the same applies to space and system states. For instance, Eulerian PDE models (Bai & Menon, 2013; Menon et al., 2004, 2006) are continuous in time, space and states, while CA-based ones are discrete in all aspects, and the Lagrangian flow model (Bilimoria, 2001) is continuous in space and state but discrete in time. Further, a model may employ a level of uncertainty within

its inputs and/or its main body, i.e. be deterministic or stochastic. For example, a cellular automaton may have deterministic or probabilistic governing rules. The CA proposed in this study is deterministic.

In this paper, focusing on the advantages of CA in time efficiency and accuracy, a model to analyze the effects of wind on delay propagation in the terminal area is proposed. The results of such an analysis can then be used in pre-tactical and tactical planning as well as decision-making processes. The rest of this paper is organized as follows. In Section 1, the types of research with a focus on weather conditions and activities that use CA in air traffic modeling are reviewed. Besides, the general structure of CA and the related explanations are given in Section 1. Section 2 is dedicated to the development of a CA model for an RNAV STAR (Area Navigation Standard Terminal Arrival Route). Subsequently, the results of simulating the proposed model for DRMMM RNAV STAR (the name of the specified route) are shown in Section 3. Finally, the final section concludes the paper.

1. Study background

Weather conditions play an important role in traffic patterns and delays. Nevertheless, due to lack of knowledge in accurate forecasting, in most cases, researchers confine to the probabilities gained from recorded data. An operational approach that accounts for weather conditions is presented in Bilimoria (2001) and Evans and Ducot (1994). Future Air Traffic Management Concepts Evaluation Tool, FACET, provides a simulation environment for evaluating novel air traffic management concepts, including air traffic control and air traffic management (NASA, 2016). FACET and its derivatives can simulate all aircraft trajectories in the American national airspace, using flight plan data, winds and aero-propulsive models of each aircraft. The Integrated Terminal Weather System, ITWS, is one of two major development projects sponsored by the FAA's Aviation Weather Development Program with focus on the airport terminal area environment. Pradeep and Wei (2017) used a microscopic approach to derive analytical equations based on flight dynamics, Base of Aircraft Data (BADA), and Total Energy Model (TEM) that give insight into the dependency of Continuous Descent Approach (CDA) and speed profile on wind speed, wind gradient, aircraft weight and type, and other factors. Young and Jerome (2013) also considered the CDA procedure in the operational phase of flight with online wind and temperature data. They proposed a design to construct 4D trajectories for optimal profile descent that is said to be computationally efficient. Although these tools are very beneficial in modeling, analyzing, studying, and also controlling traffic at aircraft-level, because of their micro approach, it may be numerically challenging to apply analytical methodologies to them in system-level applications. Another effort in considering the weather conditions in air traffic operations is done by Gardi, Sabatini, Kistan, Lim, and

Ramasamy (2015). They use a macroscopic model that provides the global distributions of pressure, temperature, winds aloft, and relative humidity, that are needed as inputs in their control model. This model is embedded in a multi-objective optimization algorithm in order to give a 4D trajectory in aircraft-level practices. In (Gardi, Marino, Ramasamy, Sabatini, & Kistan, 2016), they suggested the integration of their two multi-objective trajectory optimization algorithms into the traffic management and traffic flow management systems, with the ability to add or change the objectives as necessary. Their two algorithms are a 3D en-route variant and a 4D Terminal Maneuvering Area (TMA) variant, based on the current airspace structure. In (Callaham et al., 2001), with the aim of comparing National Air Space (NAS) performance, two normalization ways are presented: a “Weather Impacted Traffic Index”, WITI, and cluster analysis. The WITI assigns a weighted scalar value to a given day. Klein also used and refined the WITI and its counterpart, WITI-FA (Forecast Accuracy) to estimate airport delays (Klein, 2010). Compared to WITI, the WITI-FA uses forecast weather in preference to actual weather. Hoffman, Ivanescu, Shaw, and Zeghal (2003) studied airborne spacing based on constant time gaps under different operational conditions. It was shown that the maximum spacing error increased slightly with constant wind speed, but always remained within 10 seconds up to the maximum constant wind of 87 knots at a 3000 ft. altitude (FL30) and 235 knots at a 29000 ft. altitude (FL290). In other words, in the presence of constant wind at FL30 with wind speed of up to 87 knots, the aircraft can maintain their time spacing under a 10 seconds error. Delgado and Prats (2013) proposed a cruise speed reduction strategy to absorb part of the assigned airborne delay while preserving the fuel consumption level. The effect of wind on this strategy is studied, in addition to analyzing the sensitivity of the results to wind forecast errors. It is also shown that the stronger the headwind, the higher the airborne delay that can be realized. Hauf et al. (2017) forecast deviation routes through a field of storms for arriving and departing aircraft. They use storm nowcasts (i.e. detailed current weather description and forecasts in very short terms of up to 6 hours (World Meteorological Organization [WMO], 2017)) in the terminal maneuvering area of Hong Kong International Airport by using the nowcast system SWIRLS. Deviation routes are determined by the DIVSIM software package to avoid storm no-go zones.

On the other hand, Stanislaw Ulam first introduced the CA model in the 1940s while studying on crystal growth. At the same time, John Von Neumann presented a similar 2-dimensional lattice network to model self-replicating systems. These models became popular later and, in the 1960s, were studied as a particular type of dynamical systems. CAs are discrete computational tools, suitable for modeling and simulating spatiotemporal dynamics. CA includes a grid of cells. Each cell takes a state that is updated according to a governing rule at each time step. The

evolutionary history of the arrangement of these states at each time step, known as the CA configuration, shows the behavior of the system. Nagel and Schreckenberg in (Nagel & Schreckenberg, 1992) used CA for modeling traffic flow in a freeway for the first time. The so-called “NaSch” model then became a basis for traffic flow modeling with some modifications. The NaSch model has four simple steps in each time-step: acceleration, deceleration due to other vehicles, random deceleration, and vehicle position update. Biham (Biham, Middleton, & Levine, 1992) used a 2-D cellular automaton to model city and road traffic. Daganzo (1994) studied dynamical problems in the traffic flow using cellular transmission. The CA models with four simple rules proposed for traffic flow are able to explain complex traffic waves like stop-and-go, synchronized traffic phase, etc. (Chowdhury, Santen, & Schadschneider, 2000). Making an allowance for a non-Newtonian approach to traffic problems and regarding it as a self-driven system, CA became more applicable for traffic flow modeling. J.-W. Zeng et al. proposed a one-dimensional CA model to study the effect of short-range interaction between two successive vehicles due to random speed changes (J.-W. Zeng, Yang, Qian, & Wei, 2017). This model investigates the three-phase traffic flow theory in two cases: a single lane with no bottleneck that generates a synchronous flow and a single lane with an on-ramp. J. Zeng et al. devised a supervised Laplacian embedding a cellular automaton model to study a two-lane heterogeneous traffic flow that takes account for vehicles with different characteristics such as size, speed and lane-change behavior (J. Zeng, Qian, Wang, & Yang, 2017). The resulting relations between speed, density and flux show the great effect of large-scale trucks on traffic flow.

In the field of air traffic modeling, NASA was the first to use CA to develop new performance concepts and capacity increase for the future air transportation system (Barhydt, Eischeid, Palmer, & Wing, 2003). S. Amor, Tran, and Bui (2006); S. B. Amor, Dac, Bui, and Duong (2007) developed a 2D CA model in order to analyze air traffic management system performance in a portion of en-route in European airspace. They assume that controllers use speed directories and vectoring to maintain safety and resolve possible conflicts. At each time-step, an aircraft enters cell “ C_j ” according to its flight plan if the cell is available and takes Δt_{ij} time-steps to cross it. If the cell is unavailable, the aircraft will be delayed for one time-step. If the aircraft is delayed for twice in a row, it will be rerouted to one of the common neighboring sectors. An aircraft can reduce its crossing time in a sector if it was delayed. In (Kim, Abubaker, & Obah, 2005), a 2-D CA model of a self-spacing system for autonomous aircraft in en-route and arrival airspaces is proposed. This two-state directional CA, models the layout of the American National Airspace System (NAS), through a homogeneous array of cells of size $M \times N$. M and N are selected by considering the minimum separation distance, aircraft speed, and size of restricted zones. Unlike Ben Amor’s work, in

this CA, each cell can be occupied by only one aircraft. In Kim’s model, apart from the aircraft position, restricted zones and severe weather conditions are also identified in the cell state space as state “1”. Mori (2010, 2013) considered airport surface congestion as the bottleneck of an air traffic flow problem. Inspired by car traffic models, Mori focused on aircraft taxiing dynamics and took account for speed variations between aircraft. To do so, Mori modified the NaSch model to reflect the characteristics of airport traffic such as take-offs and landings, aircraft separation, aircraft dynamics, speed decision algorithms, and crossing. The model was then verified with data from Tokyo Haneda International Airport, showing that the proposed model is capable of simulating the real data in different cases with acceptable accuracy. Yu, Cao, and Zhang (2011) used a 1D optimization method to schedule an optimal aircraft landing sequence in the terminal area. He then improved this algorithm and developed a 2D CA on flight routes (He et al., 2014). With this model, an optimized landing sequence is scheduled for online application. The objective function for the optimization algorithm is the landing time error or landing time delay. It is shown that the CA model has lower computational time compared to similar models, like genetic algorithm and ant colony, and gives an improved solution for the optimization problem in terms of objective value.

Apart from the aforementioned contributions to the topic, to the extent of the authors’ knowledge and available/cited materials, this study can compensate the possible lack of resources on CA-based modeling of weather effects in the terminal area. It is also potentially a basis for future activities in this area.

1.1. Cellular automata

A cellular automaton is a discrete computational system capable of modeling and simulating complex dynamic behaviors that make it suitable for application in a vast majority of scientific fields, such as mathematics, physics, biology, etc., especially where spatiotemporal interactions are studied. Despite very simple governing rules of CAs, they exhibit an impressive range of different behaviors from order to chaos, and some classes of them have been shown to be computationally universal (i.e. capable of emulating the Turing machine (Barker-Plummer, 2016)). A CA generally has the following structure:

1. *n-Dimensional Grid.* An n -dimensional grid of cells, usually assumed to be identical, is the substrate of a CA. The size and shape of cells can affect the final emerging patterns. Each cell has a state chosen from a finite set of k possible states. The states of all cells at each time-step determine the configuration of CA at that step. As time goes by, the states change and the configuration evolves.
2. *Neighborhood.* For each cell, the number of neighbours is indicated by the interaction radius (r) for that cell, and is defined as its neighbourhood.
3. *Updating Rule (or Transition Function).* The states

of the cells are updated at each time-step, according to a specified governing rule that takes states of the neighbours of each cell into account. The updating rule can be the same for all cells, or be a function of location or time. Also, the application of the rule may be parallel (i.e. applied to all cells at once), random, or sequentially ordered (Chowdhury et al., 2000). Furthermore, updating rules can be either deterministic or stochastic. There are several ways to express an updating rule. The most intuitive way is to write down the outcome of every possible combination of neighbour states. But in a grid of dimension n , with an increasing number of possible states (k) and neighborhood radius (r), the number of these possible combinations ($|R|$) would grow rapidly, as shown in Equation 1.

$$|R| = k^{k(2r+1)^n} \quad (1)$$

Although some simplifications can be used to reduce this number, considering all possible combinations may not always be practical. In some cases, ordinary differential equations (ODE) can be used to express the updating rule, as shown in Equation 2.

$$s_i(t+1) = f(\vec{N}_i(t)), \quad (2)$$

where: $s_i(t)$ is the state of i^{th} cell at a time t , and \vec{N}_i is the vector of the states of neighbors of cell i^{th} with a neighborhood radius of r :

$$\vec{N}_i(t) = (s_{i-r}(t), \dots, s_i(t), \dots, s_{i+r}(t)). \quad (3)$$

As an example, in the case of 1D CA with $n = 1$, $k = 2$, and $r = 1$, the rule 184 (Wolfram, 2002), which is known as the traffic rule, can be expressed as shown in Equation 4.

$$s_i(t+1) = (\overline{s_{i-1}(t)}s_i(t)) + (s_i(t)s_{i+1}(t)), \quad (4)$$

where $\overline{s_i(t)}$ is the negation of $s_i(t)$, i.e. if $s_i(t) = 1$, then $\overline{s_i(t)} = 0$, and vice versa. In many cases, splitting the rule in each step into some sub-steps with If-Then phrases is better for understanding and implementing it.

4. *Boundary Conditions.* Since the definition of neighbours for boundary cells may be different from other cells, some imaginary cells need to be assumed, the state of which can dramatically affect the results of the model. The periodic boundary condition is one of the most commonly used assumptions. The result of this assumption is a ring-shaped lattice in a 1D CA and a toroidal-shaped lattice in a 2D CA. One may also consider other existing boundary conditions such as open, reflective, or fixed conditions.

Since 1981, by introducing “Elementary Cellular Automata”, Stephan Wolfram has extensively studied the properties of CAs (Wolfram, 2002). An elementary CA is a 1D grid of identical cells with $k = 2$, i.e. each cell can

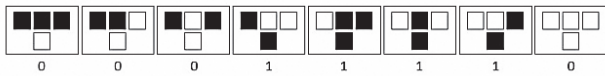


Figure 2. Demonstration of Rule 30

have one of the two states, say, $\{0, 1\}$ or $\{on, off\}$. The neighborhood of each cell is presented by its immediate cells on its left and right, that is $r = 1$. In this case, there will be $2^3 = 8$ possible state combinations for a given cell whose resulting state is defined by the update rule. An illustration of the rule is shown in Figure 2, where the first row shows the eight possible combinations, and the second row is the state of the middle cell in the next time-step. Wolfram considered all different outcomes for the combination described above, which results in $2^8 = 256$ rules. He named all possible rules by an 8-bit binary number from rule-0 to rule-255 (e.g. the rule in Figure 2 is $30 = (00011110)_2$). He then defined the four classes of a 1D CA, according to their emerging behavior, starting from different initial conditions (Wolfram, 2002). Class one includes those rules that evolve nearly all initial patterns quickly into a stable and homogenous state. The resulting state for nearly all initial patterns under the rules in class two have stable or oscillating structures. Figure 3 illustrates examples of classes three and four. Rule 30 and rule 90, belonging to class three (two rules on the left), have pseudo-random or chaotic structures for nearly all initial patterns.

For rules in class four, a more complex behavior may result in relatively simple initial patterns. Local structures and patterns, like those in class two, may emerge and survive for long periods. In Bouarfa, Blom, Curran, and Everdij (2013), the authors use the definition of emergence derived from the above presented classification in CA in order to study air transportation behavior as a complex socio-technical system.

2. STAR-CA model

In this paper, the influence of headwind and tailwind in the terminal area on arrival times to the waypoints for all flights in the traffic flow is considered. The wind is reflected in the model as a change in aircraft speed at each time-step. Speed changes relative to wind speed and

direction are extracted from (Hoffman et al., 2003). A 1D array of identical rectangular cells is used to model the arrival phase of a flight on an RNAV STAR, starting from the last waypoint on the flight plan that corresponds to the end of the en-route phase, to the point where the aircraft starts an instrument approach or is vectored by air traffic control. RNAV routes are defined with the purpose of optimized use of the airspace. Assisted by Global Navigation Satellite Systems (GNSS) such as the Global Positioning System (GPS) created by the United States or Galileo navigation system created by the European Union, route design is no longer restricted to the position of ground navigational aids. Here, aircraft are presumed to have been cleared for the route, i.e. are well equipped and capable of following the RNAV STAR route. In this model, each cell in the array may be either occupied by an aircraft or empty, with the exception of waypoints that are assigned to holding patterns that may be occupied by n_{max} number of aircraft, where n_{max} is the maximum number of aircraft that can be inside a holding pattern at the same time. The size of the cells is chosen so that the aircraft moves from a cell to the next immediate cell at the slowest permissible speed in each section of the route in one time-step. The neighborhood radius equals the number of cells that the aircraft can cross at its highest allowed speed in one time-step. Similar to the modified *NaSch* model used in road traffic, the transition rule consists of four sub-steps: acceleration, safety deceleration, wind effect on speed (corresponding to the randomization step in the *NaSch* model) and position update. It is desirable that the aircraft fly the route at the highest allowed speed while maintaining the safe separation minima. It is the Air Traffic Control's (ATC's) responsibility to guarantee this safe separation between flights by utilizing suitable advisories such as speed change, vectoring, and directing aircraft to holding patterns. The present model suggests speed advisories and holding patterns for the arrival phase of flight.

In this model, at each time step, for each occupied cell, first, the gap between the occupying aircraft and its preceding flight is checked (left path of the flowchart in Figure 4). If there were enough room for acceleration, the following aircraft would speed up. The amount of speed change is first restricted by the aircraft's ability to increase its speed in one time-step, and then by the maximum

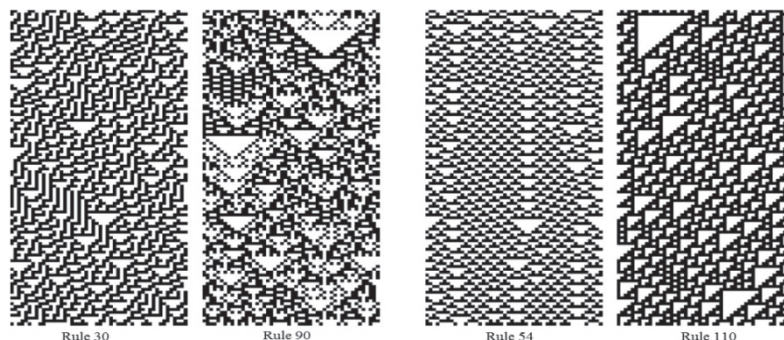


Figure 3. CAs with Rule 30 and 90 (left) and Rules 54 and 110 (right), showing different emerging behaviors

allowed speed specified by ATC or in published charts. If the following aircraft is closer to the leading aircraft than the separation minima, then, it should slow down. Again, the speed decrease is limited by the aircraft’s ability to decelerate and the stall speed of the aircraft at the flying altitude. If the distance to the leading aircraft equals the separation minima, the aircraft will not change its speed. This speed is the True Air Speed (TAS) of the aircraft. In order to calculate the aircraft location, the ground speed is needed, which is the sum of the TAS and wind speed. After updating the ground speed, if the separation minima are violated, then the ATC directs the following aircraft to the holding pattern, where it remains for a specified period. The speed is calculated by Equation 5 as follows.

$$TAS(t+1) = \begin{cases} \max(TAS(t) + \delta V^+, V_{max}) & d_{req} > V_{max} \delta t; \text{acceleration} \\ \min(TAS(t) - \delta V^-, V_{min}) & d_{req} < V_{min} \delta t; \text{deceleration} \\ TAS(t) & \text{else ; normal,} \end{cases} \quad (5)$$

where: $TAS(t)$ is the True Air Speed of aircraft at time t , δV^+ is the possible speed increment according to aircraft engine performance at the current altitude in one time-step, and V_{max} is the highest allowed speed according to the RNAV STAR procedure. δV^- is the affordable deceleration of the aircraft at flying altitude, V_{min} is the minimum allowed speed according to the RNAV STAR procedure or aircraft performance (i.e. its stall speed margin), δt is one time-step, d_{req} is the required safe distance separation between flights.

Subsequently, the ground speed is calculated from Equation 6. The ground speed is the aircrafts’ actual speed relative to the ground. If the aircraft is confronted with a headwind, the instruments on the aircraft overvalue the true speed. Therefore, to calculate the real speed, one has to subtract the wind speed. In the case of tailwind, the instruments underestimate the speed and the wind speed is added to calculate the ground speed.

$$V(t+1) = TAS(t+1) \pm W(t), \quad (6)$$

where $+W$ is the speed of the tailwind and $-W$ is the speed of headwind. It should be noted that, in this study, a field of constant speed wind is considered, so the value of $W(t)$ is the same for all affected cells at time step t .

If, with the updated ground speed, the safe distance is violated, the aircraft will be directed to a holding pattern, since it cannot further reduce its speed (Equation 7). The speed in the holding pattern, $V_{holding}$, is given in the RNAV procedure.

$$V(t+1) = \begin{cases} V_{holding} & d_{req} < V(t+1) \delta t \\ V(t+1) & \text{else} \end{cases} \quad (7)$$

Finally, the aircraft’s position, $P(t)$, is updated by equation 8.

$$P(t+1) = P(t) + V(t+1) \delta t. \quad (8)$$

It is important to indicate that the effect of the wind on the vertical and lateral path of the aircraft is neglected and the cell array is aligned with the actual path. With this assumption, only the longitudinal deviation of the flight from the nominal path is presented. The procedure described above is presented in Figure 4.

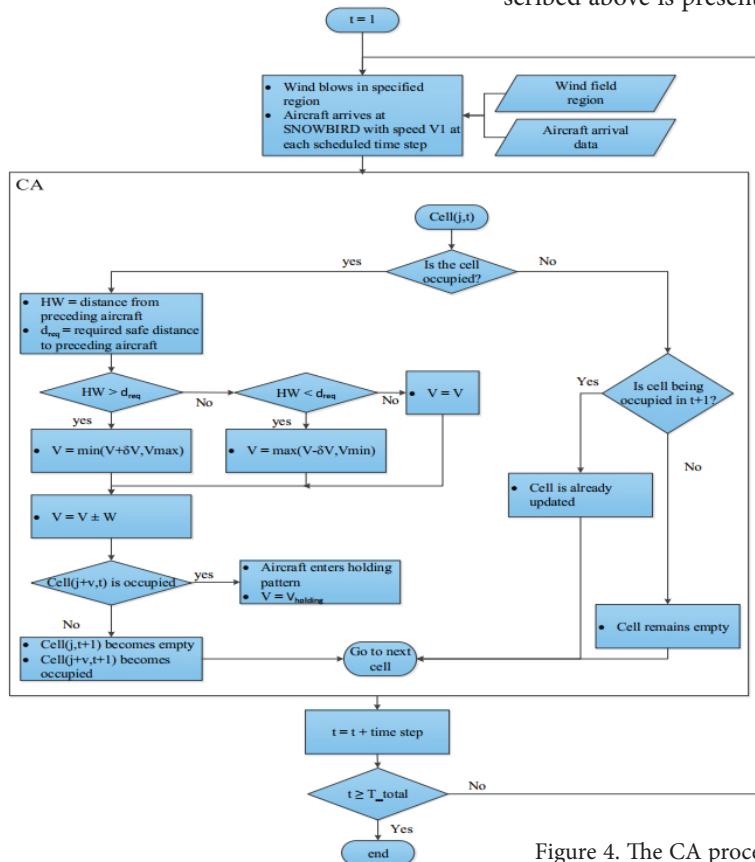


Figure 4. The CA procedure presented in this paper

3. Simulation results

For simulation purposes, an RNAV STAR route in *Hartsfield-Jackson Atlanta International Airport* (ATL) is modeled. This airport is one of the busiest airports in the US and in the world. As a result, delays are expected to propagate rapidly. One branch of the EERZA STAR route, from EERZA to DRMMM, is selected (lower line in Figure 5). The length of this route is 101 nautical miles. The normal speed in descent phase is 300 *knots*, which is taken as V_{max} at the top of EERZA. At the DRMMM waypoint, the altitude reaches 13000 *ft*. and the maximum speed is reduced linearly to 280 *knots*. According to real arrival traffic data in ATL, on average, 105 flights per hour land at the airport, 30% of which arrive from the northwest quarter of the terminal airspace. Since the authors do not have access to a real distribution of these flights between existing routes and during the time, a uniform distribution is assumed. This leaves 20 flights/hour that enter the DRMMM STAR route, 50% of which enter from the EERZA waypoint. The arrival time of these flights is also distributed uniformly in one hour; i.e. an aircraft arrives at EERZA every 6 minutes. All aircraft are assumed to belong to the heavy category, hence, the minimum required time headway between each pair equals 90 *seconds*.

Although the longitudinal separation in descent and approach phases is complicated, and is a function of many operational variables, as a rule of thumb, 90 seconds can be said to be equivalent to a 6~7 nm distance headway (d_{req}) between two heavy aircraft. The operational performance of the aircraft is modeled by a point mass performance model, and the speed change dynamics is neglected. Hence, it is assumed that the speed changes occur

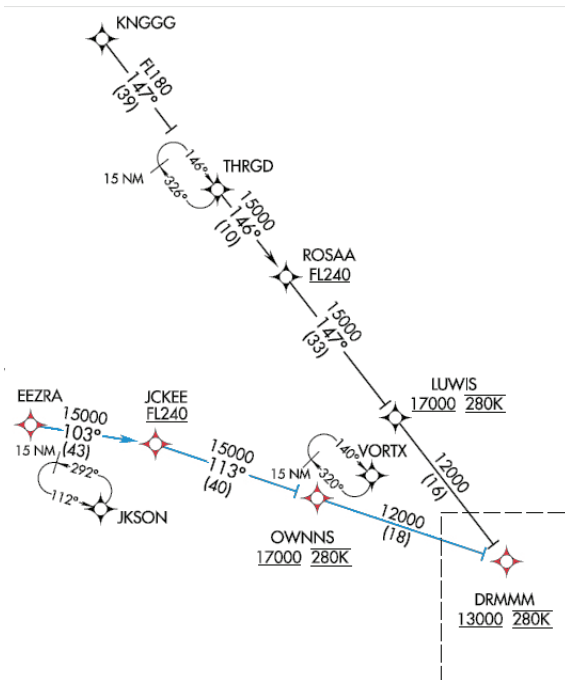


Figure 5. The DRMMM RNAV STAR

within one time-step and $\delta V^{\pm} = \pm 1 \frac{cell}{time\ step}$ and $V_{holding}$ is chosen so that the holding time equals 4 minutes. The index used to verify the model is the rate of flights arriving at the DRMMM waypoint, given the number of flights entering the airspace via the EERZA waypoint under a no-wind condition. For this purpose, the number of flights arriving at the EERZA and DRMMM waypoints was monitored during different intervals throughout a week (Flight-radar, 2018). Then, the model uses the rate of arrivals at the EERZA waypoint as the input, and the output arrival rate at the DRMMM waypoint is compared to the one in the gathered data. It should be noted that this data verifies the main structure of the model algorithm, and, since the wind effect is considered through the speed changes of the aircraft, the structure can be used for a windy case as well. Nevertheless, the authors acknowledge that having the model verified with wind data would improve the accuracy level of the model. Such a consideration will be covered in the next steps of this work. Table 1 illustrates the results of comparing these data. It is evident that the model tends to overestimate the delay in all cases. The reason may be due to the simplifications employed in the model, such as the simple point mass performance for aircraft and simplified ATC dynamics. On the other hand, the online data used for verification is not complete. Yet, this level of accuracy can be fairly good in the pre-tactical phase of traffic control.

In the scheme that was explained, six scenarios are simulated. In the first scenario, a constant speed stationary headwind field is placed between JCKEE and OWNNS waypoints for one hour from $t = 25\ min$ to $t = 85\ min$. Although tailwinds are more constraining in the landing phase due to safety issues, headwinds delay the flights by decreasing the ground speed and are considered in this scenario. The speed of the wind is assumed as $W = 40\ knots$, which is a normal wind speed aloft (Aviation Weather Center, 2017). In the second scenario, the same wind field moves toward the DRMMM waypoint. In this case, the size of the so-called windy area is constant for simplification. The traffic flow is exposed to the wind field for one and a half hour from $t = 25\ min$ to $t = 115\ min$. In the third scenario, a simple dynamic is added to the wind, so that the wind changes with time and location along the route. For 30 minutes, from $t = 25\ min$ to $t = 55\ min$, the wind speed is $W = 45\ knots$ and the effective

Table 1. Real and simulated arrival rates at DRMMM

| Simulation Duration (min) | 60 | 120 | 180 | 240 |
|---|------|------|------|------|
| Real Arrival Rate at EERZA (flight/hour) | 9 | 10 | 12 | 12 |
| Real Arrival Rate at DRMMM (flight/hour) | 8 | 9.5 | 11.3 | 11.5 |
| Simulated Arrival Rate at DRMMM (flight/hour) | 7 | 8 | 10 | 11.2 |
| Error (%) | 12.5 | 15.8 | 11.7 | 2.2 |

range is located 35 cells away from the EEZRA waypoint with a length of 40 cells. The speed is then decreased to $W = 35 \text{ knots}$ between $t = 55 \text{ min}$ to $t = 85 \text{ min}$. It returns to its first value again for the next 30 minutes. It should be noted that the wind speed data are simplified from (Aviation Weather Center, 2017) and that the changes are hypothetical to show the effect of a variable speed wind on delay propagation. In the fourth scenario, the number of aircraft entering the airspace is doubled to analyze the delay propagation behavior in heavier traffic. It should be noted that, in these four scenarios, the aircraft arrive at EEZRA at fixed time headways, which is not realistic. A more genuine arrival rate is simulated in scenario 5 and scenario 6, where normal traffic flow (10 flights/hour) and heavy traffic flow (20 flights/hour) arrive at the EEZRA waypoint with random arrival time headways, respectively. The wind field is the same as in scenario 4. Table 2 summarizes these characteristics for the arrival rates and their distribution over time, as well as the spatiotemporal characteristics of the wind field in each scenario.

In Figure 6, the results of a two-hour simulation for all scenarios are shown. Each line shows the location of an aircraft along the route. The slope of the line represents the ground speed of the aircraft. The top left diagram (Figure 6a) refers to the first scenario. It can be seen that, since the wind field affects all aircraft similarly, the pattern is adjusting accordingly. As a result, all aircraft are delayed by the same amount, and delays are not accumulated. In addition, the delay effect does not permeate upstream, i.e. after $t = 85 \text{ min}$, when the wind speed is set to $W = 0 \text{ knots}$, the next flight arrives at the DRMMM waypoint within its estimated time of arrival (ETA) and with no further delays. The simulation of scenario one with heavier traffic, i.e. shorter arrival intervals at the EEZRA waypoint, shows that this property is independent to the aircraft density. This property does not hold for the second scenario where, after $t = 115 \text{ min}$, the next aircraft ETAs increase. The time space diagram of this scenario is shown in Figure 6b. The diagram on the bottom left (Figure 6c) shows the results of simulating scenario 3, where aircraft enter a variable speed wind field. It can be seen that more aircraft are affected upstream

of the traffic flow when the wind speed is higher. Comparing this diagram with that of scenario 4 (Figure 6d) shows that the delay propagation pattern does change severely with increasing density of flights.

In Figure 6e, for the 5th scenario, it can be seen that the randomness in arrival times at EEZRA slightly affects the headways, which are interpreted from the distance between lines. This effect increases with arrival rate, as in Figure 6f, showing the same diagram for scenario 6.

Figure 7a depicts the average ground speed of all flights that have reached the DRMMM waypoint in scenario 4. Here, the minimum speed is forced equal to 4 cell/min (260 knots). The optimum operating speed equals 5 cell/min (280 knots), and the aircraft can accelerate up to 6 cell/min (300 knots). It should be noted that the dynamics of speed change is not considered in this study, without sinking accuracy. In other words, we assume that speed increase/decrease take place instantly. A normal undisturbed flight (like flight number 1) would have an average speed of 5.5 cell/min , and it takes it 17 minutes to get from the EEZRA waypoint to DRMMM. In Figure 7b, a histogram of the average speed for scenario 4 shows that nearly 60% of the flights fly slower due to the headwind field that affects half of the route for 75% of the simulation time. The average ground speed of flights and their histogram for scenario 6 are shown in Figure 7c and 7d respectively. The speed increase between flights 10 and 15 that occurs between $t = 22 \text{ min}$, and $t = 40 \text{ min}$, is due to the increased time headway between these flights, which causes a diminution of delay propagation upstream. The speed drop between flights 22 to 25, which is completely in opposition to that of scenario 4, is due to the change in arrival rate that coincides with the change in headwind speed at $t = 75 \text{ min}$. In other words, the comparison of Figure 7a and 7c clarifies the effect of arrival rate on the propagation of the perturbations like the wind to the upstream flow.

The resulting belatedness in both scenarios 4 and 6 is reflected in the flight times, as shown in Figure 8a and 8b, respectively. The average flight time for all flights in this route is 22.48 minutes with a standard deviation of 4.6 minutes. The considerably high deviation is due to the implementation method of the wind field. Here, the wind speed increment is rather high, which causes harsh changes in aircraft speed and, consequently, flight times. It is also notable that, as a consequence of increased average speed in scenario 6, the average flight time is lower, and the downstream disturbance due to the wind has a weaker effect on upstream traffic, compared to scenario 4. This outcome can later be used in assigning Scheduled Time of Arrivals (STA) at waypoints along flight segments.

The slow-downs and speed-ups induce inconsistencies in flight headways that increase controllers' workload. With an orderly arrival rate at the EEZRA waypoint, a reduction in headway between flights leads to an increase in aircraft density in the route, defined by the number of aircraft flying along the route between EEZRA and

Table 2. The main features of the simulated scenarios

| | Arrival Traffic Flow (AC/h) | Arrival Time Distribution | Wind Field |
|------------|-----------------------------|---------------------------|---------------------------|
| Scenario 1 | 10 | Uniform | Stationary Constant Speed |
| Scenario 2 | 10 | Uniform | Moving Constant Speed |
| Scenario 3 | 10 | Uniform | Moving Variable Speed |
| Scenario 4 | 20 | Uniform | Moving Variable Speed |
| Scenario 5 | 10 | Random | Moving Variable Speed |
| Scenario 6 | 20 | Random | Moving Variable Speed |

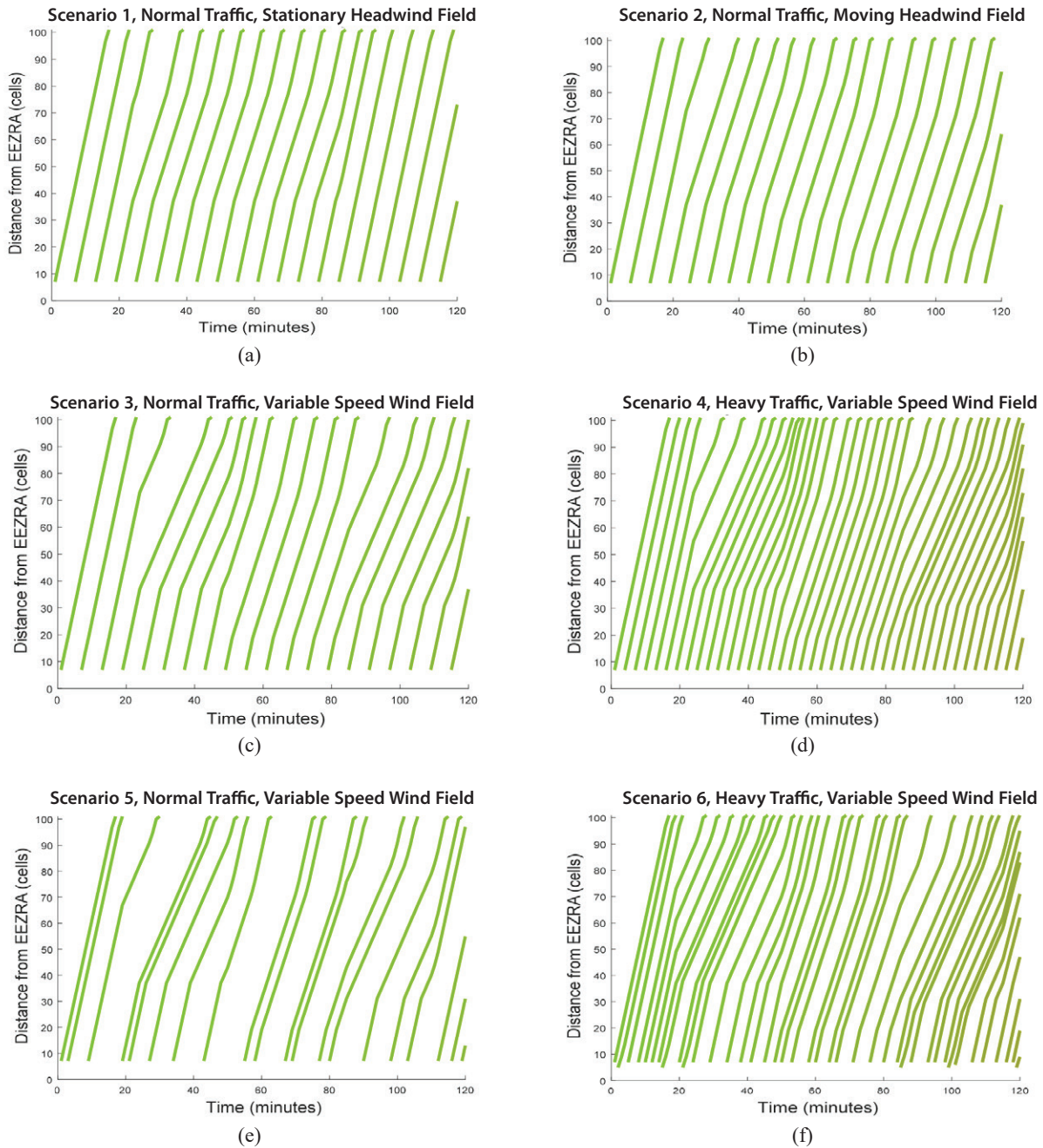


Figure 6. Time-space diagram of the six simulated scenarios: a – normal traffic flow entering stationary headwind field with constant speed; b – normal traffic flow entering a moving headwind field with constant speed; c – normal traffic flow entering a variable speed headwind field; d – heavy traffic flow entering a variable speed headwind field; e – normal traffic with random arrival time entering a variable speed headwind field; f – heavy traffic with random arrival time entering a variable speed headwind field

DRMMM, including those in holding patterns. In Figure 9a, the average distance headway for each aircraft is shown. The nominal headway for an undisturbed flight to its preceding one is 16 cells, and the minimum safe headway is 6 cells. An increase in average headway means that the aircraft has fallen behind its desired headway. It should be noted that, since headways are measured relative to the preceding aircraft, changes in headway do not necessarily reflect a deviation from schedule. Figure 9b, shows time changes in a number of aircraft flying along the route.

It can be seen that the presence of the wind field causes an increase in aircraft density that can be translated into an increase in controllers' workload. To show the effect of arrival rate once more, the same diagrams for scenario 6 are presented in Figure 9c and 9d, respectively. As expected, the headway diagram illustrates the randomness in arrival times. The red line shows the desired average headways in the absence of wind, and the blue line is the simulation result when the traffic flow is exposed to the variable speed headwind field. To be consistent with speed

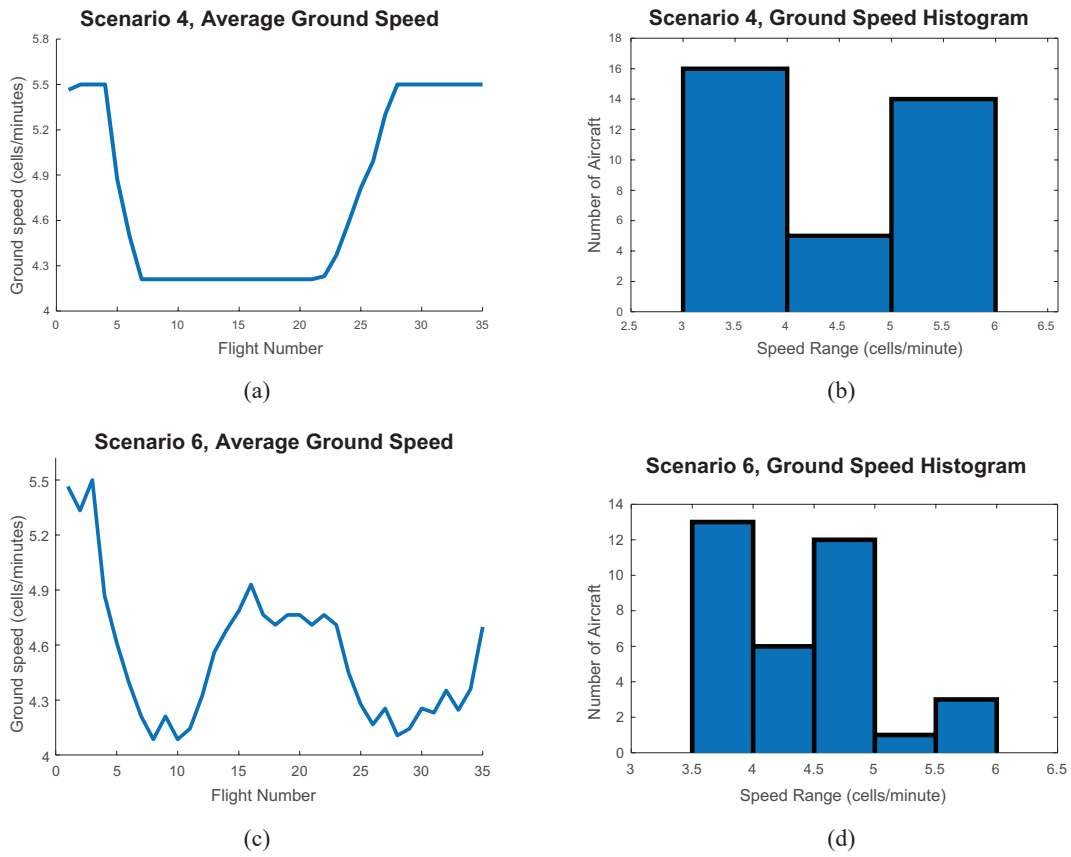


Figure 7. Comparison of ground speeds in scenario 4 and 6: a – average ground speed for each flight in scenario 4; b – histogram of average ground speed for all flights in scenario 4; c – average ground speed for each flight in scenario 6; d – histogram of average ground speed for all flights in scenario 6

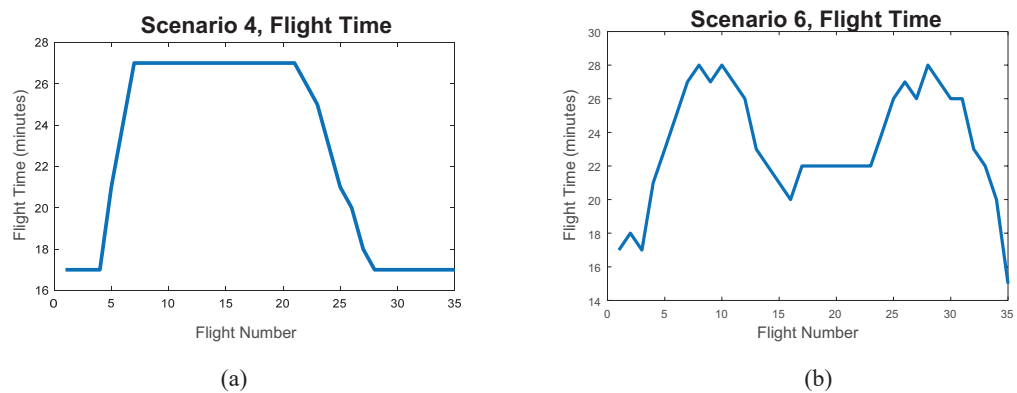


Figure 8. The flight time of aircraft from EEZRA to DRMMM in: a – scenario 4; b – scenario 6

and flight time results, it is shown that with the decrease in arrival rate for flights 15–25, the headway deviation is also decreased. This effect can also be seen in Figure 9d, where the density of flights in the route remains constant, but is higher compared to that of scenario 4 (Figure 9b).

As mentioned, time efficiency is the beneficial property of a CA model that makes it suitable for online ap-

plications, such as the tactical phase of air traffic control processes. With an average run time of 2.9 seconds and a standard deviation of 0.3 seconds, the proposed model simulates a two-hour operation. What is more, simulation of scenario 4 with the same run time shows the model's insensitivity to the flow rate within the limits of airspace capacity.

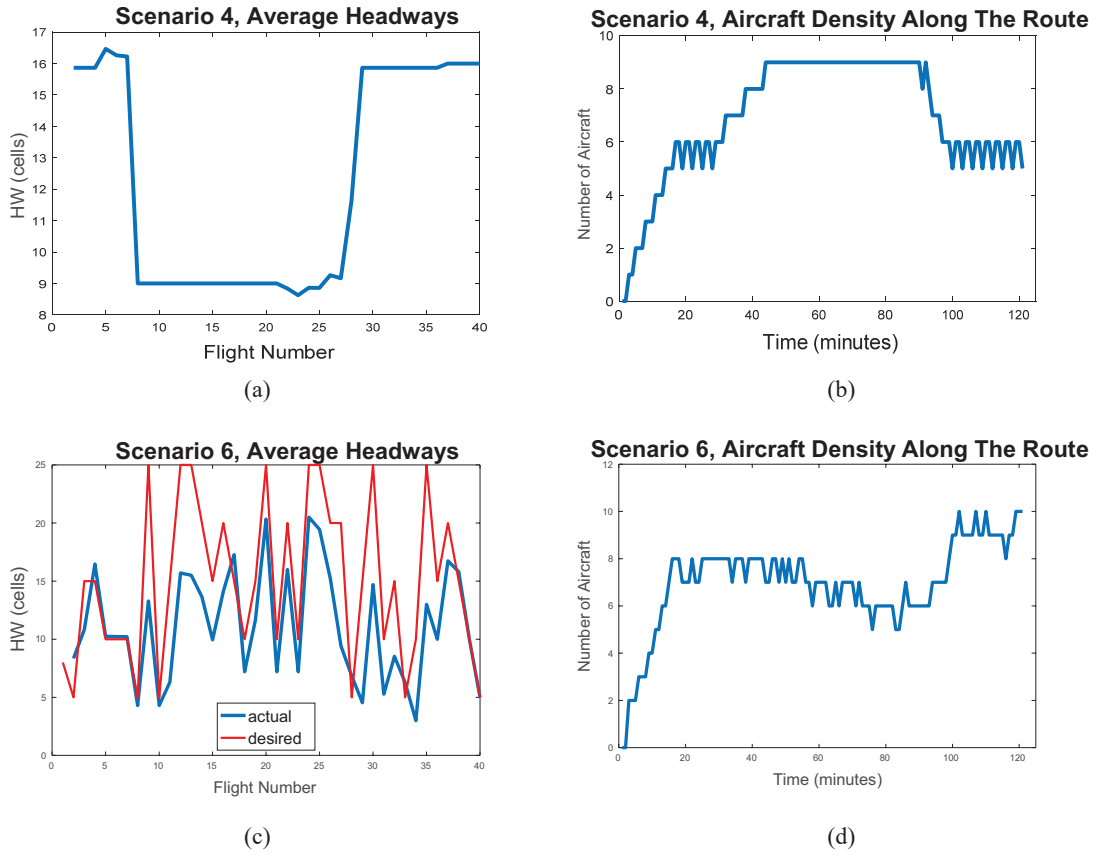


Figure 9. Average distance headway of flights (left) and aircraft density along the route (right) in scenario 4

It is worth noting that, neglecting vertical and lateral effects of the wind on the flight path in order to simplify the analysis, results in a 2 to 15 percent loss of accuracy and extensiveness of the model. Normally, during an unforeseen tailwind, the aircraft will accelerate up to a specified airspeed to keep up with the reference trajectory and Vertical Navigation (VNAV) allows the aircraft to rise up to a specified range above the path. If VNAV can no longer maintain the aircraft within 150 ft. of the path without further acceleration, VNAV switches from VNAV PTH to VNAV SPD, resets the target airspeed, and ignores the nominal VNAV flight path. Similarly, during an unforeseen headwind and with inactive auto-throttle, the aircraft will fly below the path to stop the deceleration. Once VNAV can no longer maintain the aircraft within the range without further deceleration, VNAV switches from VNAV PTH to VNAV SPD, resets the target airspeed, and ignores the nominal VNAV flight path. This can be modeled by a 2D CA that represents a plane in which a vertical descent path is projected. In order to take account of lateral deviations of the flight due to cross-winds and turbulence, the model can be extended into a 3D array of cells.

Conclusions

In the presented manuscript, the behavior of delay propagation in the presence of headwind in the terminal area

was studied based on a 1D CA model. The developed CA model was verified by real online data in a windless scenario. The index used to verify the model was the arrival rate of the flights at the end waypoint of the route, given the real arrival rate at the entrance. In this regard, we adopted an RNAV STAR route in one of the busiest airports in the US (ATL); afterwards, one branch of the DRMMM STAR route, from EERZA to DRMMM was selected for the simulations. Using the proposed model and six simulated scenarios, we presented the effects of changes in wind properties and changes in the arrival rate of the traffic on the delay propagation from downstream to upstream of the traffic flow. Afterwards, a statistical analysis, based on the average and the histogram of the ground speeds, was conducted. Based on the presented outcomes, the model exhibited an acceptable level of accuracy (a 3–15% loss of accuracy), with worthy time and computational efficiency (an average run time of 2.9 seconds for a two-hour operation) as discussed in a greater detail. Henceforth, this combination could be integrated for use with automated air traffic control and management systems in the tactical phase, where a fast analysis of the flow behavior under different perturbations, such as windy weather conditions, is needed. The CA models based on a 2D/3D array of cells for considering the lateral deviations of the flight due to cross-winds and turbulence are the topics of upcoming investigations.

References

- Airbus. (2013). *Future journeys 2013–2032. Global market forecast*. Retrieved from <https://www.airbusgroup.com>
- Amor, S., Tran, D., & Bui, M. (2006, December). *Investigating air traffic control dynamics using random cellular automata*. Paper presented at the Eurocontrol Innovative Research Workshop & Exhibition. Bretigny-sur-Orge, France.
- Amor, S. B., Dac, H. T., Bui, M., & Duong, V. (2007). *Simulating dynamic ATM network effects using cellular automata*. Paper Presented at the Proceedings of the European Conference on Complex Systems. ECCS. Dresden. Germany.
- Aviation Weather Center. (2017). *Forecast winds and temps aloft*. Retrieved from <https://aviationweather.gov/windtemp>
- Bai, X., & Menon, P. (2013, August). *Optimal terminal area flow control using eulerian traffic flow model*. Paper presented at AIAA Guidance, Navigation, and Control (GNC) Conference. Boston, MA.
- Barhydt, R., Eischeid, T. M., Palmer, M. T., & Wing, D. J. (2003). *Regaining Lost Separation in a Piloted Simulation of Autonomous Aircraft Operation*. Paper Presented at the 5th USA/Europe Air Traffic Management R&D Seminar. Budapest, Hungary.
- Barker-Plummer, D. (2016). Turing machines. In E. N. Zalta (Ed.), *The stanford encyclopedia of philosophy* (Winter 2016 Ed.). Metaphysics Research Lab, Stanford University.
- Bayen A. M., Raffard, R. L., & Tomlin, C. J. (2004). *Eulerian network model of air traffic flow in congested areas*. Paper presented at the Proceedings of the American Control Conference, Boston, MA. <https://doi.org/10.23919/ACC.2004.1384733>
- Biham, O., Middleton, A. A., & Levine, D. (1992). Self-Organization and a dynamical transition in traffic-flow models. *Physical Review A*, 46(10), 3. <https://doi.org/10.1103/PhysRevA.46.R6124>
- Bilimoria, K. D., Sridhar, B., Chatterji G. B., Sheth, K. S., & Grabbe S. R. (2001). FACET: Future ATM concepts evaluation tool. *Air Traffic Control Quarterly*, 9(1), 1-20. <https://doi.org/10.2514/atcq.9.1.1>
- Bouarfa, S., Blom, H. A., Curran, R., & Everdij, M. H. (2013). Agent-based modeling and simulation of emergent behavior in air transportation. *Complex Adaptive Systems Modeling*, 1(1), 15. <https://doi.org/10.1186/2194-3206-1-15>
- Callaham, M., Dearmon, J., Cooper, A., Goodfriend, J., Moch-Mooney, D., & Solomos, G. (2001, December). *Assessing NAS performance: Normalizing for the effects of weather*. Paper Presented At The 4th Usa/Europe Air Traffic Management R&D Symposium, Santa-Fe.
- Chowdhury, D., Santen, L., & Schadschneider, A. (2000). Statistical physics of vehicular traffic and some related systems. *Physics Reports*, 329(4), 199-329. [https://doi.org/10.1016/S0370-1573\(99\)00117-9](https://doi.org/10.1016/S0370-1573(99)00117-9)
- Daganzo, C. F. (1994). The cell transmission model: a dynamic representation of highway traffic consistent with the hydrodynamic theory. *Transportation Research B*, 28(4), 269-287. [https://doi.org/10.1016/0191-2615\(94\)90002-7](https://doi.org/10.1016/0191-2615(94)90002-7)
- Delgado, L., & Prats, X. (2013). Effect of wind on operating-cost-based cruise speed reduction for delay absorption. *IEEE Transactions on Intelligent Transportation Systems*, 14(2), 918-927. <https://doi.org/10.1109/TITS.2013.2246864>
- Evans, J. E., & Ducot, E. R. (1994). The Integrated Terminal Weather System (ITWS). *The Lincoln Laboratory Journal*, 7(2), 449-474.
- Federal Aviation Administration. (2017, August 29). *Weather delay. NextGen*. Retrieved from <https://www.faa.gov/nextgen/programs/weather/faq/>
- Flightradar. (2018). Live air traffic. Retrieved from <https://www.flightradar24.com/data/airports/atl/arrivals>
- Gardi, A., Marino, M., Ramasamy, S., Sabatini, R., & Kistan, T. (2016). *4-Dimensional trajectory optimisation algorithm for air traffic management systems*. Paper presented at the IEEE/AIAA 35th Digital Avionics Systems Conference (DASC). <https://doi.org/10.1109/DASC.2016.7778083>
- Gardi, A., Sabatini, R., Kistan, T., Lim, Y., & Ramasamy, S. (2015). *4 dimensional trajectory functionalities for air traffic management systems*. Paper presented at the Integrated Communication, Navigation, And Surveillance Conference (ICNS), Herdon, VA, USA. <https://doi.org/10.1109/ICNSURV.2015.7121246>
- Gomez, R. (2007). *Next generation air traffic management, boeing's view*.
- Hauf, T., Hupe, P., Sauer, M., Rokitsky, C.-H., Lang, J., Sacher, D., ... Sakiew, L. (2017). Aircraft route forecasting under adverse weather conditions. *Meteorologische Zeitschrift*, 26(2), 189-206. <https://doi.org/10.1127/metz/2016/0786>
- He, Y., Cai, K., Li, Y., & Xiao, M. (2014). *An improved cellular-automaton-based algorithm for real-time aircraft landing scheduling*. Paper presented at the Seventh International Symposium on Computational Intelligence And Design (ISCID). Hangzhou, China. IEEE. <https://doi.org/10.1109/ISCID.2014.243>
- Hoffman, E., Ivanescu, D., Shaw, C., & Zeghal, K. (2003, June). *Analysis of constant time delay airborne spacing between aircraft of mixed types in varying wind conditions*. Paper presented at the USA/Europe Air Traffic Management R&D Seminar, Budapest, Hungary.
- Jacobsen, R. (2000). *NASA airspace systems program*. Paper presented at the Virtual Airspace Modeling and Simulation Project, Technical Interchange Meeting.
- Kim, C., Abubaker, K., & Obah, O. (2005). *Cellular automata modeling of en route and arrival self-spacing for autonomous aircrafts*. Paper presented at the 50th Annual Meeting of Air Traffic Controllers Association.
- Klein, A. (2010). *Airport delay prediction using weather-impacted traffic index (WITI) model*. Paper presented at the IEEE/AIAA 29th Digital Avionics Systems Conference (DASC), Salt Lake City, UT, USA. <https://doi.org/10.1109/DASC.2010.5655493>
- Matsukidaira, J., & Nishinari, K. (2004). Euler-Lagrange correspondence of generalized burgers cellular automaton. *International Journal of Modern Physics C*, 15(04), 507-515. <https://doi.org/10.1142/S0129183104005917>
- Menon, P. K., Sweriduk, G. D., & Bilimoria, K. D. (2004). New approach for modeling, analysis, and control of air traffic flow. *Journal of Guidance, Control, and Dynamics*, 27(5), 737-744. <https://doi.org/10.2514/1.2556>
- Menon, P. K., Sweriduk, G. D., Lam, T., Diaz, G., & Bilimoria, K. D. (2006). Computer-aided eulerian air traffic flow modeling and predictive control. *Journal Of Guidance, Control, and Dynamics*, 29(1), 12-19. <https://doi.org/10.2514/1.13496>
- Mori, R. (2010). *Modeling of aircraft surface traffic flow at congested airport using cellular automata*. Paper presented at the Proceedings of the 4th International Conference on Research in Air Transportation (ICRAT), Budapest, Hungary.
- Mori, R. (2013). Aircraft ground-taxiing model for congested airport using cellular automata. *IEEE Transactions on Intelligent Transportation Systems*, 14(1), 180-188. <https://doi.org/10.1109/TITS.2012.2208188>
- Nagel, K., & Schreckenberg, M. (1992). A cellular automaton model for freeway traffic. *Journal De Physique I*, 2(12), 2221-2229. <https://doi.org/10.1051/jp1:1992277>

- NASA. (2016). Future air traffic management concepts evaluation tool (FACET). Retrieved from <https://software.nasa.gov/software/arc-14653-1>
- Pasaoglu, C., Baspinar, B., Ure, N. K., & Inalhan, G. (2015). Hybrid systems modeling and automated air traffic control for three-dimensional separation assurance. *Proceedings of the Institution of Mechanical Engineers, Part G: Journal of Aerospace Engineering*, 230(9), 1788-1809. <https://doi.org/10.1177/0954410015619443>
- Pradeep, P., & Wei, P. (2017). *Predictability, variability and operational feasibility aspect of CDA*. Paper presented at the IEEE Aerospace Conference. Big Sky, MT, USA. <https://doi.org/10.1109/AERO.2017.7943728>
- Schumer, S. C. E. (2008). *Your flight has been delayed again: flight delays cost passengers, airlines and the U.S. economy billions*. Retrieved from https://www.jec.senate.gov/public/index.cfm/democrats/2008/5/your-flight-has-been-delayed-again_1539
- Sun, D., Strub, I. S., & Bayen, A. M. (2007). Comparison of the Performance of Four Eulerian Network Flow Models for Strategic Air Traffic Management. *Networks and Heterogeneous Media*, 2(4), 569-595. <https://doi.org/10.3934/nhm.2007.2.569>
- Wolfram, S. (2002). *A new kind of science*: Wolfram Media.
- World Meteorological Organization. (2017). *Nowcasting*. Retrieved from <http://www.wmo.int/pages/prog/amp/pwsp/nowcasting.htm>
- Yang, B.-J., & Menon, P. (2015). Real-time air traffic flow estimation in the terminal area. *Journal of Aircraft*, 52(3), 778-791. <https://doi.org/10.2514/1.C032701>
- Young, S.-Y., & Jerome, K. (2013). *Optimal profile descent with 4-D trajectory*. Paper presented at the Integrated Communications, Navigation And Surveillance Conference (ICNS). Herndon, VA, USA. <https://doi.org/10.1109/ICNSurv.2013.6548601>
- Yu, S.-P., Cao, X.-B., & Zhang, J. (2011). A real-time schedule method for aircraft landing scheduling problem based on cellular automation. *Applied Soft Computing*, 11(4), 3485-3493. <https://doi.org/10.1016/j.asoc.2011.01.022>
- Zeng, J.-W., Yang, X.-G., Qian, Y.-S., & Wei, X.-T. (2017). Research on three-phase traffic flow modeling based on interaction range. *Modern Physics Letters B*, 31(35), 1750328. <https://doi.org/10.1142/S0217984917503286>
- Zeng, J., Qian, Y., Wang, M., & Yang, Y. (2017). On supervised graph laplacian embedding Ca Model & Kernel construction and its application. *Journal of Experimental & Theoretical Artificial Intelligence*, 29(1), 81-89. <https://doi.org/10.1080/0952813X.2015.1132259>
- Zhang, H., Xu, Y., Yang, L., & Liu, H. (2014). Macroscopic model and simulation analysis of air traffic flow in airport terminal area. *Discrete Dynamics in Nature and Society*. Article ID 741654. <https://doi.org/10.1155/2014/741654>

List of acronyms

| | |
|-----|--|
| ATL | Hartsfield-Jackson Atlanta International Airport |
| ATM | Air Traffic Management |
| CA | Cellular Automaton |
| CDA | Continuous Descent Approach |
| ETA | Estimated Time of Arrival |

| | |
|-------------|--|
| FAA | Federal Aviation Administration |
| FACET | Future Air Traffic Management Concepts Evaluation Tool |
| FL | Flight Level |
| GNSS | Global Navigation Satellite System |
| GPS | Global Positioning System |
| ITWS | Integrated Terminal Weather System |
| NAS | National Air Space |
| NaSch Model | Nagel and Schreckenberg Model |
| RNAV | Area Navigation |
| STA | Scheduled Time of Arrival |
| STAR | Standard Terminal Arrival Route |
| TAS | True Air Speed |
| TMA | Terminal Maneuvering Area |
| VNAV | Vertical Navigation |
| WITI | Weather Impacted Traffic Index |
| WITI-FA | Weather Impacted Traffic Index-Forecast Accuracy |

List of symbols

| | |
|---------------|---|
| d_{req} | Standard Separation Minima |
| δV^- | Possible Speed Decrease per Time-Step |
| δV^+ | Possible Speed Increase per Time-Step |
| i | n-Dimensional Vector of i^{th} Cell Position |
| k | Number of Possible States |
| \vec{N} | Vector of Neighbors' States |
| n | Grid Dimension |
| $P(t)$ | Aircraft Position at Time t |
| r | Neighborhood Radius |
| R | Number of Possible Rules |
| $s_i(t)$ | State of i^{th} Cell at Time t |
| $TAS(t)$ | True Air Speed of Aircraft at Time t |
| $V(t)$ | Aircraft Ground Speed at Time t |
| $V_{holding}$ | Aircraft Speed in Holding Pattern |
| V_{max} | Maximum Permissible Speed |
| V_{min} | Minimum Permissible Speed |
| W | Wind Speed |